Coulomb breakup mechanism of neutron-halo nuclei in a time-dependent method

T. Kido,[1] K. Yabana,[2] and Y. Suzuki[2]
[1]*Graduate School of Science and Technology, Niigata University, Niigata 950-21, Japan*
[2]*Department of Physics, Niigata University, Niigata 950-21, Japan*
(Received 26 December 1995)

The mechanism of the Coulomb breakup reactions of the nuclei with neutron-halo structure is investigated in detail. A time-dependent Schrödinger equation for the halo neutron is numerically solved by treating the Coulomb field of a target as an external field. The momentum distribution and the post-acceleration effect of the final fragments are discussed in a fully quantum mechanical way to clarify the limitation of the intuitive picture based on the classical mechanics. The theory is applied to the Coulomb breakup reaction of ^{11}Be+ ^{208}Pb. The breakup mechanism is found to be different between the channels of $j^{\pi}=1/2^{-}$ and $3/2^{-}$, reflecting the underlying structure of ^{11}Be. The calculated result reproduces the energy spectrum of the breakup fragments reasonably well, but explains only about a half of the observed longitudinal momentum difference. [S0556-2813(96)01905-X]

PACS number(s): 25.60.Gc, 25.70.De, 25.70.Mn

I. INTRODUCTION

The neutron-halo structure has been observed systematically [1] in light neutron-rich nuclei near the neutron drip line. A large Coulomb breakup cross section has been observed for the neutron-halo nucleus in reactions on a heavy target nucleus [2], which indicates that a significant amount of $E1$ strength exists at low excitation energy region of the neutron-halo nucleus [3]. Since stable nuclei do not have such a strong $E1$ distribution at low excitation energy, this unusual feature of the neutron-halo nucleus has attracted much attention. The origin of the strong $E1$ distribution is still controversial: It may be a resonant character due to the vibration of the halo neutron against a core nucleus [4]. Or it may be understood from an analogy of the strong $E1$ transitions known in ^{9}Be, ^{11}Be, and ^{13}C where a single nucleon is weakly coupled to a core nucleus [5]. A recent argument suggests that the low-lying $E1$ strength of the light halo nuclei is not considered the vibrational state [6].

Recent experiments of the Coulomb breakup reactions, ^{11}Li+ ^{208}Pb [7] and ^{11}Be+ ^{208}Pb [8], have observed a significant longitudinal momentum difference between the halo neutron(s) and the core nucleus. The momentum difference has been explained in terms of the Coulomb postacceleration effect by assuming a direct breakup mechanism. In this mechanism the breakup is assumed to occur instantaneously at the closest approach point between the projectile and target nuclei. After the breakup of the projectile nucleus, the target Coulomb field accelerates only the core nucleus, and causes the momentum difference between the neutron and the core nucleus. If the breakup proceeds through a resonant state of the projectile nucleus, the core nucleus and the halo neutron move together during its lifetime and the postacceleration effect should become small. The observation of the longitudinal velocity difference is thus recognized as a direct evidence for the nonresonant character of the $E1$ strength at low excitation energy.

The postacceleration effect is not explained in the lowest order perturbation treatment of the Coulomb excitation. The evaluation of higher order effects is not easy because the final states involve continuum states. Several theoretical approaches have been proposed to understand the postacceleration effect, including a classical treatment of the breakup reaction [9], a distorted-wave Born approach [10], a simplified treatment of the higher order perturbations [11], and a coupled-channel approach with discretized continuum states [12]. Contrary to these approaches, some groups have investigated the time evolution of the projectile nucleus by solving a time-dependent Schrödinger equation on mesh points of space and time variables [13,14].

In our previous paper [14] we studied the Coulomb breakup of ^{11}Be and found large transverse and small longitudinal momentum differences between the neutron and the ^{10}Be nucleus. The result was understood in the picture of a free-particle breakup mechanism which is in contrast to the direct breakup mechanism. However, the reproduction of the experimental momentum difference remained an open problem. In this paper we extend the previous calculation to a more realistic case by including the spin-orbit interaction between the neutron and the core nucleus. A full three-dimensional dynamical calculation has also been done in [13(b)] assuming a simple internal Hamiltonian. No investigation has, however, so far been performed to clarify the roles of the ls potential and the level structure of excited states. We first analyze the mechanism of the Coulomb breakup quantum mechanically for various cases of the neutron-core Hamiltonian. The results are discussed in comparison with the intuitive arguments based on the classical mechanics. The usefulness and limitation of the classical arguments is made clear. We then analyze the Coulomb breakup reaction of ^{11}Be+ ^{208}Pb [8] with a realistic choice of the potential between the halo neutron and ^{10}Be. We show that the breakup mechanism is sensitive to the structure of the excited states of the projectile and that the inclusion of the spin-orbit interaction is very important to reproduce the observed features quantitatively.

In Sec. II we formulate the quantum-mechanical treatment of the Coulomb breakup reaction using the time-dependent Schrödinger equation. The method of calculating the time evolution of the wave function is briefly explained. In Sec.

III the theory is applied to various cases of the halo nucleus to discuss the limitation of the classical arguments for the Coulomb breakup reaction and to reveal the characteristics of the quantum aspect. The Coulomb breakup of ^{11}Be on a ^{208}Pb target is analyzed in Sec. IV. A brief summary is given in Sec. V.

II. FORMULATION

We consider the Coulomb breakup reaction of the nucleus with neutron-halo structure. The projectile of the halo nucleus is assumed to consist of a single neutron and a core nucleus. The core nucleus is treated as a structureless particle and binds the neutron weakly by an appropriate potential. We describe the reaction in the projectile rest frame where the center of mass of the projectile is put at the origin of the coordinate. The time development of the wave function, $\Psi(\mathbf{r},t)$, of the relative motion between the neutron and the core nucleus is described by the following time-dependent Schrödinger equation:

$$i\hbar\frac{\partial}{\partial t}\Psi(\mathbf{r},t)=\{H(\mathbf{r})+V_{\rm ext}(\mathbf{r},t)\}\Psi(\mathbf{r},t), \tag{1}$$

where $H(\mathbf{r})=-(\hbar^2/2\mu)\nabla^2+V(\mathbf{r})$ is the internal Hamiltonian describing the relative motion between the halo neutron and the core nucleus. We assume that the projectile moves along a straight line trajectory with a constant velocity. The target nucleus exerts a Coulomb potential $V_{\rm ext}(\mathbf{r},t)$ on the projectile. The potential is treated as a time-dependent external field in the projectile rest frame,

$$V_{\rm ext}(\mathbf{r},t)=\frac{Z_C Z_T e^2}{|[m_n/(m_n+M_C)]\mathbf{r}+\mathbf{b}+\mathbf{v}t|}-\frac{Z_C Z_T e^2}{|\mathbf{b}+\mathbf{v}t|}. \tag{2}$$

Here $\mathbf{b}$ is the impact parameter which specifies the straight line trajectory, $\mathbf{v}$ is the incident velocity of the projectile, and Z_T and Z_C are the charge numbers of the target and core nucleus, respectively. The masses of the neutron and the core nucleus are denoted by m_n and M_C, respectively.

The wave function is expanded in partial waves as

$$\Psi(\mathbf{r},t)=\sum_{lm}\frac{u_{lm}(r,t)}{r}Y_{lm}(\hat{\mathbf{r}}). \tag{3}$$

When the internal Hamiltonian $H(\mathbf{r})$ includes the spin-orbit interaction, it is convenient to couple the spin of the neutron with the relative orbital angular momentum l to the total angular momentum j. Since the generalization to such a case is straightforward, we develop the formulation by assuming the wave function of Eq. (3).

We descretize the time variable in a step Δt, and represent the wave function of the nth time step as $\Psi^{(n)}(\mathbf{r})$. The wave function of $(n+1)$th time step is calculated by the following formula:

$$\Psi^{(n+1)}(\mathbf{r})\simeq e^{-iH(\mathbf{r})\Delta t/\hbar}e^{-iV_{\rm ext}(\mathbf{r},t)\Delta t/\hbar}\Psi^{(n)}(\mathbf{r}). \tag{4}$$

The radial part of the wave function of the nth step is denoted as $u_{lm}^{(n)}(r)$. The time development is then achieved by two successive procedures. First, the development due to the external field $V_{\rm ext}(\mathbf{r},t)$ is approximated by

$$u_{lm}^{(n+1/2)}(r)=u_{lm}^{(n)}(r)-i\Delta t/\hbar\sum_{l'm'}\langle lm|V_{\rm ext}(\mathbf{r},t)|l'm'\rangle u_{l'm'}^{(n)}(r). \tag{5}$$

The evaluation of the matrix element in Eq. (5) is done by expanding the external field into multipoles. Next the time development by the internal Hamiltonian is performed separately for each angular momentum channel, lm, by using the following approximation:

$$u_{lm}^{(n+1)}(r)=\frac{1-i(\Delta t/2\hbar)h_l(r)}{1+i(\Delta t/2\hbar)h_l(r)}u_{lm}^{(n+1/2)}(r), \tag{6}$$

with

$$h_l(r)=-\frac{\hbar^2}{2\mu}\frac{d^2}{dr^2}+\frac{\hbar^2 l(l+1)}{2\mu r^2}+V_l(r). \tag{7}$$

To obtain $u_{lm}^{(n+1)}(r)$ from $u_{lm}^{(n+1/2)}(r)$, we discretize the radius variable r on mesh points of an equal spacing and employ the Crank-Nicolson formula [15] using a three-point formula for the second-order differential operator.

The time evolution is calculated according to the above prescription from an initial wave function, $\Psi(\mathbf{r},t=-\infty)=\phi_0(\mathbf{r})$, which is the ground-state wave function of the internal Hamiltonian. The breakup component of the wave function is obtained by eliminating all the bound state components of the Hamiltonian

$$|\Psi_{\mathbf{b}}^{\rm BU}(\mathbf{r},t)\rangle=\left(1-\sum_{i\in{\rm bound}}|\phi_i\rangle\langle\phi_i|\right)|\Psi(\mathbf{r},t)\rangle. \tag{8}$$

Here the subscript $\mathbf{b}$ is kept to stress that the time evolution of the wave function is calculated for each impact parameter of the external field.

The momentum distribution of the relative motion between the neutron and the core nucleus after the breakup is obtained by

$$\frac{dP_{\rm BU}(\mathbf{b},\mathbf{k})}{d\mathbf{k}}=\lim_{t\to\infty}|\langle\mathbf{k}|\Psi_{\mathbf{b}}^{\rm BU}(\mathbf{r},t)\rangle|^2, \tag{9}$$

where $|\mathbf{k}\rangle$ represents the plane wave state. The integration of Eq. (9) over $\mathbf{k}$ yields the Coulomb breakup probability, $P_{\rm BU}(b)=\lim_{t\to\infty}\langle\Psi_{\mathbf{b}}^{\rm BU}(\mathbf{r},t)|\Psi_{\mathbf{b}}^{\rm BU}(\mathbf{r},t)\rangle$, for a given $\mathbf{b}$. Integrating $P_{\rm BU}(b)$ over the impact parameter vector yields the total Coulomb breakup cross section.

The breakup cross section can be expressed as a function of the relative motion energy E between the neutron and the core nucleus as follows:

$$\frac{d\sigma_{\rm BU}}{dE}=2\pi\int_{b_{\rm min}}^{\infty}dbb\int d\mathbf{k}\delta(E_{\mathbf{k}}-E)\frac{dP_{\rm BU}(\mathbf{b},\mathbf{k})}{d\mathbf{k}}, \quad (10)$$

where $E_{\mathbf{k}}=\hbar^2k^2/2\mu$. The convergence of the integral in Eq. (10) is very slow with respect to the impact parameter. Furthermore the calculation of the relative momentum distribution requires a long time step for large impact parameters. To circumvent this difficulty, we divide the integration interval of b to two parts, $[b_{\rm min},b_s]$ and $[b_s,\infty]$, and in the latter interval employ the first-order perturbation theory to calculate the energy distribution. The value of b_s is chosen in such a way that the first-order perturbation theory (PT) and the time-dependent (TD) calculation give approximately the same energy distribution at $b=b_s$. Equation (10) is then recast to

$$\frac{d\sigma_{\rm BU}}{dE}=\frac{d\sigma_{\rm BU}^{\rm (TD)}}{dE}+\frac{d\sigma_{\rm BU}^{\rm (PT)}}{dE}. \quad (11)$$

The second term of Eq. (11) is expressed in a closed form by using the perturbation theory. For this aim we use the breakup probability distribution which is obtained in the first-order perturbation theory,

$$\frac{dP_{\rm BU}^{\rm (PT)}(b)}{dE}=\frac{16\pi}{9}\frac{Z_T^2e^2}{(\hbar v)^2}\left(\frac{\xi}{b}\right)^2[K_0^2(\xi)+K_1^2(\xi)]\frac{dB(E1)}{dE}, \quad (12)$$

where K_0 and K_1 are the modified Bessel functions and $\xi=bE/\hbar v$. By integrating Eq. (12) over the impact parameter in the interval $[b_s,\infty]$, we obtain

$$\frac{d\sigma_{\rm BU}^{\rm (PT)}}{dE}=\frac{16\pi}{9}\frac{Z_T^2e^2}{(\hbar v)^2}2\pi\xi_sK_0(\xi_s)K_1(\xi_s)\frac{dB(E1)}{dE}, \quad (13)$$

where $\xi_s=b_sE/\hbar v$.

The $B(E1)$ strength function in Eqs. (12) and (13) is defined by

$$\begin{aligned}\frac{dB(E1)}{dE}&\equiv\sum_{Mi}|\langle\phi_i|D_{1M}|\phi_0\rangle|^2\delta(E_i-E)\\&\quad+\sum_M\int d\mathbf{k}|\langle\phi_{\mathbf{k}}|D_{1M}|\phi_0\rangle|^2\delta(E_{\mathbf{k}}-E)\\&=\sum_M\langle\phi_0|D_{1M}^{\dagger}\delta(\hat{H}-E)D_{1M}|\phi_0\rangle\\&=-\frac{1}{\pi}\sum_M{\rm Im}\left\langle\phi_0\left|D_{1M}^{\dagger}\frac{1}{E-H+i\varepsilon}D_{1M}\right|\phi_0\right\rangle\end{aligned} \quad (14)$$

with the dipole operator D_{1M} defined by

$$D_{1M}=-\frac{Z_C}{A_C+1}erY_{1M}(\hat{\mathbf{r}}), \quad (15)$$

where A_C is the mass number of the core nucleus. The wave functions ϕ_i and $\phi_{\mathbf{k}}$ of Eq. (14) are the bound excited states and continuum states of the Hamiltonian $H(\mathbf{r})$ and E_i and $E_{\mathbf{k}}$ are the corresponding eigenvalues, respectively. To calculate the $B(E1)$ strength function we rewrite Eq. (14) in a time-dependent form,

$$\begin{aligned}&\frac{dB(E1)}{dE}\\&=\frac{3}{\pi\hbar}{\rm Re}\left\langle\phi_0\left|D_{10}^{\dagger}\int_0^{\infty}dte^{(i/\hbar)(E+i\varepsilon)t}e^{-(i/\hbar)Ht}D_{10}\right|\phi_0\right\rangle\\&=\frac{3}{\pi\hbar}{\rm Re}\int_0^{\infty}dte^{(i/\hbar)(E+i\epsilon)t}\langle\phi_0|D_{10}^{\dagger}|\psi(t)\rangle,\end{aligned} \quad (16)$$

where the ground state is assumed to have $l=0$. The wave function $\psi(t)=e^{-(i/\hbar)Ht}D_{10}\phi_0$ satisfies the time-dependent Schrödinger equation with the Hamiltonian $H(\mathbf{r})$ and its initial wave function $\psi(0)$ is equal to $D_{10}\phi_0$. By solving the time-dependent Schrödinger equation without an external field, it is possible to obtain the wave function $\psi(t)$ and then calculate the $B(E1)$ strength function according to Eq. (16). It is straightforward to generalize Eq. (16) to the case where the spin-orbit potential is included.

III. QUANTUM-MECHANICAL ANALYSIS OF COULOMB BREAKUP PROCESS

To elucidate the breakup mechanism of a neutron-halo nucleus, we investigate the breakup process for various choices of the internal Hamiltonian $H(\mathbf{r})$. Before showing calculated results, we first discuss typical intuitive pictures for the breakup mechanism based on the classical mechanics. They include (1) a direct breakup mechanism, (2) a resonant breakup mechanism, (3) a free-particle breakup mechanism. In the direct breakup mechanism, the neutron is assumed to be removed suddenly from the core nucleus when the projectile nucleus approaches the point closest to the target nucleus. After the breakup occurs, only the core nucleus is accelerated by the target Coulomb field. The relative momentum between the neutron and the core nucleus is finite both for the longitudinal and transverse directions. When the projectile nucleus has such a resonance state that can be excited from the ground state by the target Coulomb field, the resonant breakup process may become important and the breakup may proceed dominantly by way of the resonance. If the lifetime of the resonance is long enough, the neutron and the core nucleus would move together for a long time before the breakup occurs. In such an extreme case there is no difference in the relative momentum between the neutron and the core nucleus. In the last case of free-particle breakup mechanism we consider the limiting case where the binding energy of the neutron is extremely small. Then the neutron and the core nucleus behave independently during the reaction. The core nucleus moves along the Rutherford trajectory, while the halo neutron, receiving no Coulomb force from the target, moves on the straight line. In the end the core nucleus receives the momentum only in the transverse direction. The momentum difference between the neutron and the core nucleus arises only in the transverse direction.

TABLE I. The classical estimates of the average longitudinal and transverse momenta, $\langle k_{\parallel}\rangle$ and $\langle k_{\perp}\rangle$, of the relative motion after the projectile nucleus fragments into the neutron and the core nucleus by the target Coulomb field. Three reaction mechanisms are classified and characterized by the classical momentum $k_c=[m_n/(m_n+M_C)]Z_TZ_Ce^2/\hbar bv$, where Z_Ce (Z_Te) is the charge of the core (target) nucleus, m_n and M_C are the masses of the neutron and the core nucleus, respectively, v is the incident velocity of the projectile nucleus, and b is the impact parameter. The zero momentum for the resonant breakup is the limiting case of a long lifetime.

	Resonant	Direct	Free particle
$\langle k_{\parallel}\rangle$	0	k_c	0
$\langle k_{\perp}\rangle$	0	k_c	$2k_c$

Table I summarizes the momentum differences for the three cases discussed above.

It is not clear how well the above classical arguments are quantitatively correct, though they are easily accepted intuitively. In what follows we show results of the quantum-mechanical calculations for various cases of the neutron-core interactions for which the above-mentioned reaction mechanisms are expected to be manifest.

We choose various parameters for the study of the breakup reaction of ^{11}Be on a ^{208}Pb nucleus performed at the incident energy of 72 MeV/nucleon [8]. Hence the projectile nucleus of ^{11}Be has the incident velocity of $v/c=0.37$. By choosing the reaction plane to be an x-z plane, the target nucleus moves on the straight line $\mathbf{R}_T(t)=(b,0,-vt)$ in the projectile rest frame. The impact parameter b is fixed to $b=12$ fm in the present section. The radius variable r is taken up to 800 fm and it is descretized with the mesh size of $\Delta r=0.4$ fm. The time step $\Delta t/\hbar=0.01$ MeV^{-1} is used for calculating the time development of the wave function. The Schrödinger equation is solved for the time interval of $-10\leqslant t/\hbar\leqslant 10$ MeV^{-1}. At the initial and final stages of the calculation, the target nucleus is apart from the projectile's center-of-mass coordinate by about 750 fm in the longitudinal direction.

We assume that the $1/2^+$ ground state of the ^{11}Be nucleus is described with a single neutron-halo structure in the $1s$ orbit around the inert ^{10}Be core. The potential between the neutron and the core nucleus is taken to be a spherical Woods-Saxon potential. The spin-orbit interaction is turned off in the calculation presented in this section. The radius and diffuseness parameters of the potential are fixed to $R=2.67$ fm and $a=0.6$ fm, whereas the depth of the potential is treated as a variable parameter to investigate the breakup mechanism. The partial waves up to $l=4$ are included in the expansion of Eq. (3). The contribution of higher partial waves is found to be negligible. The target Coulomb field of Eq. (2) is expanded in multipoles around the projectile's center of mass, and the dipole and quadrupole multipoles are included in the calculation. The dipole field plays a dominant role in the present system. The contribution of the quadrupole field is found to be small.

The average value of the relative momentum between the neutron and the core nucleus is calculated by the following formula:

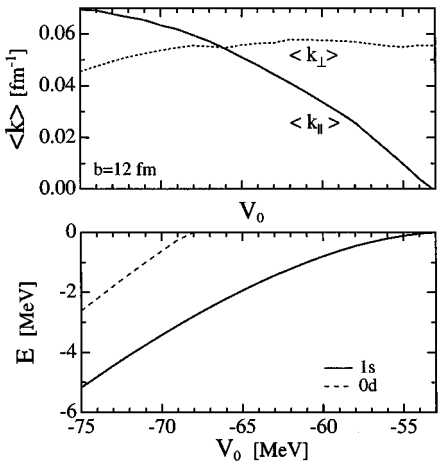

FIG. 1. The average values of the longitudinal (solid curve) and the transverse (dashed curve) momentum difference between the neutron and the core nucleus as a function of the neutron-core potential depth V_0. The impact parameter b is set 12 fm. The energies of the bound orbits from the neutron threshold are shown in the lower part.

$$\langle \mathbf{k}\rangle=\lim_{t\to\infty}\frac{\langle \Psi_{\mathbf{b}}^{\mathrm{BU}}(\mathbf{r},t)|-i\nabla|\Psi_{\mathbf{b}}^{\mathrm{BU}}(\mathbf{r},t)\rangle}{\langle \Psi_{\mathbf{b}}^{\mathrm{BU}}(\mathbf{r},t)|\Psi_{\mathbf{b}}^{\mathrm{BU}}(\mathbf{r},t)\rangle}. \tag{17}$$

Similarly the average values of the longitudinal and transverse momentum differences, $\langle k_{\parallel}\rangle$ and $\langle k_{\perp}\rangle$, are defined by the breakup component $\Psi_{\mathbf{b}}^{\mathrm{BU}}(\mathbf{r},t)$. We use the convention that the longitudinal and transverse directions indicate the z and x directions, respectively.

A. Dependence on the neutron binding energy

To discuss the validity of the classical arguments summarized in Table I, we first show the result of calculation obtained by changing the neutron-core potential depth V_0 of $l=0$ channel. The value of V_0 is varied to understand the dependence of the breakup reaction mechanism on the binding energy of the halo neutron of the $1s$ orbit. The potential depth of other channels, denoted V_p, is set the same as V_0. The $0p$ orbit is always bound below the $1s$ orbit, and there is no resonant nor bound excited state which can be excited from the ground state by the dipole field. The halo nucleus considered in this subsection is thus a very simple system, and excited to the continuum directly by the Coulomb field.

Figure 1 displays the magnitude of $\langle k_{\parallel}\rangle$ and $\langle k_{\perp}\rangle$ values as a function of V_0. The lower part of Fig. 1 shows the binding energy of the $1s$ orbit. As the binding becomes weaker, the longitudinal momentum difference decreases and approaches zero in the vanishing binding energy, while the transverse momentum difference increases slightly. This result is consistent with the free-particle breakup picture. However, the transverse relative momentum is always smaller than the value, $2k_c=0.092$ fm^{-1}, which is expected from the classical argument. On the other hand, in the strong binding case, both of the longitudinal and transverse momentum differences are finite and close to the value of $k_c=0.046$ fm^{-1}, which is just expected from the direct breakup picture. These calculations including both weak and strong

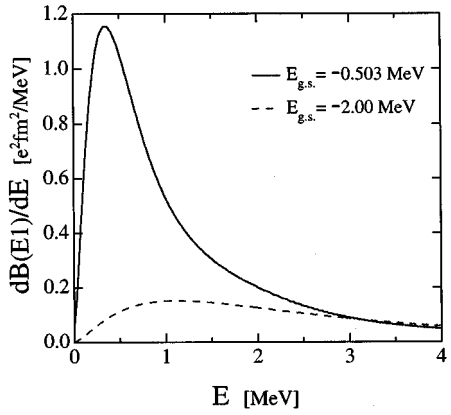

FIG. 2. The $B(E1)$ strength as a function of the energy E of the relative motion between the neutron and the core nucleus. Two choices of the neutron-core potential depth V_0 are made to locate the $1s$ ground state at -0.503 MeV ($V_0=-58.3$ MeV) and -2.00 MeV (-65.2 MeV).

binding cases indicate that the breakup mechanism of the neutron-halo nucleus, whose binding energy is typically less than 1 MeV, proceeds between the two mechanisms of the direct and free-particle breakup. The free-particle picture becomes more suitable with the decreasing binding energy of the halo neutron.

We show in Fig. 2 the $B(E1)$ strength as a function of the neutron-core relative energy. The value of ε of Eq. (16) is set 0.01 MeV. The $B(E1)$ strength function is closely related to the energy spectrum of the breakup cross section [see Eq. (13)]. The nonperturbative effect gives only a small effect on the energy spectrum of the cross section [14,13(b)]. The $B(E1)$ strength is shown for two cases of the ground-state energy: $E=-2.00$ MeV ($V_0=-65.2$ MeV), and $E=-0.503$ MeV ($V_0=-58.3$ MeV). The latter value is chosen to fit the empirical neutron separation energy of ^{11}Be. No resonance exists in p wave for both cases. Therefore the peak in the $B(E1)$ strength which appears at low excitation energy in case of $E=-0.503$ MeV has nothing to do with any resonant character. We see that the energy spectrum of the $B(E1)$ strength is very sensitive to the neutron binding energy. Since the breakup probability is sensitive to the $E1$ strength at low excitation energy, the breakup cross section is also sensitive to the neutron binding energy.

B. Dependence on the level structure of excited states

Here we investigate how the breakup mechanism depends on the structure of the excited states of the halo nucleus. For this purpose we employ the angular momentum (l-) dependent neutron-core potential. The potential depth of $l=0$ channel is fixed to $V_0=-58.3$ MeV in order to fit the energy of the $1s$ orbit to $E_0=-0.503$ MeV, the ground-state energy of ^{11}Be from the $n+^{10}$Be threshold. The value of V_p is now treated as a variable parameter. As shown in the lower part of Fig. 3, there is a bound $0p$ state when $V_p\leqslant -31.3$ MeV. In the case of -33.2 MeV$<V_p<-31.3$ MeV, the bound $0p$ state appears between the $1s$ ground state and the neutron threshold. This $0p$ state is excited by the dipole field in the breakup reaction. In case of -31.3 MeV $\leqslant V_p\leqslant -30$ MeV a p-wave resonance with a long lifetime appears in the continuum.

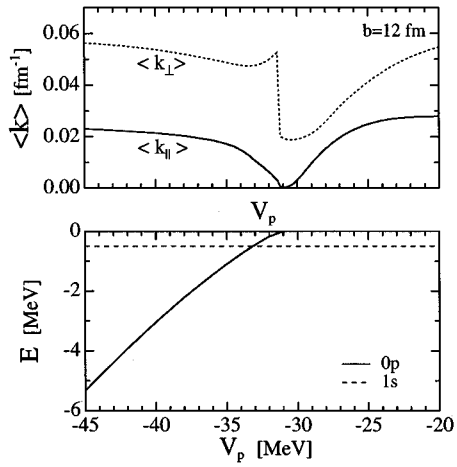

FIG. 3. The average values of the longitudinal (solid curve) and the transverse (dashed curve) momentum difference between the neutron and the core nucleus as a function of the neutron-core potential depth V_p of $l\neq 0$ channel. The impact parameter b is set 12 fm. The solid curve in the lower part shows the energy of the bound $0p$ orbit from the neutron threshold. The energy of the $1s$ orbit is fixed to -0.503 MeV as indicated by dashed line in the lower part.

Figure 3 plots the average relative momentum as a function of V_p. As expected, when the resonance state exists both of the average relative momenta in the longitudinal and transverse directions are very small. It is important to note, however, that the transverse momentum remains finite even when the resonance energy is very close to zero and thus its lifetime becomes very long. This indicates that the resonant breakup mechanism is too much oversimplified. When the potential depth is deep enough to have a bound excited state, the average relative momentum shows quite different behavior between the longitudinal and transverse directions. The longitudinal momentum difference is still very small and changes continuously from the case where the excited state is the resonance. In contrast with this the transverse momentum difference increases discontinuously from the resonance case. These results of small longitudinal and large transverse relative momenta might suggest that the breakup proceeds through the free-particle breakup mechanism in this case. There is, however, no physical reason that the free-particle breakup mechanism is correct. This is because two breakup processes occur when there is a bound excited state: One is the direct breakup to the continuum. The other is the breakup via the bound excited state. The latter process apparently does not fit in with the free-particle breakup mechanism. At present we do not have a simple explanation for the discontinuous change in the transverse momentum difference and the continuous behavior in the longitudinal momentum difference which show up when the excited $0p$ orbit crosses the threshold. When the $0p$ orbit is bound more deeply ($V_p<-35$ MeV), or is in the nonresonant continuum ($V_p>-25$ MeV), the momentum differences become similar to those of the previous subsection ($V_p=V_0=-58.3$ MeV, see Fig. 1), that is, $\langle k_\parallel\rangle=0.026$ fm^{-1} and $\langle k_\perp\rangle=0.059$ fm^{-1}, and are rather insensitive to the potential depth.

The $B(E1)$ strength function is compared in Fig. 4 for two choices of V_p: One is $V_p=-30.0$ MeV where the $0p$ resonance appears at about 0.2 MeV. The other is

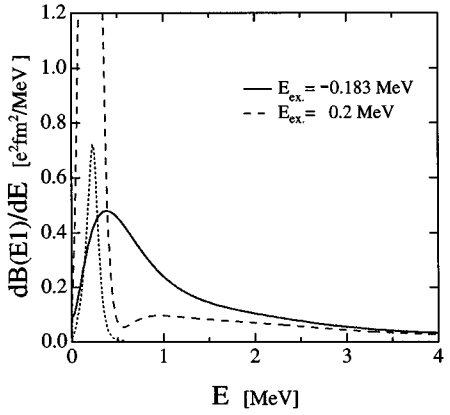

FIG. 4. The $B(E1)$ strength as a function of the energy E of the relative motion between the neutron and the core nucleus. Two choices of the neutron-core potential depth V_p of $l\neq 0$ channel are made to locate the $0p$ orbit at -0.183 MeV ($V_p=-32.0$ MeV) and 0.2 MeV (-30.0 MeV). The dotted curve indicates the strength reduced to one-tenth of the result shown by dashed curve.

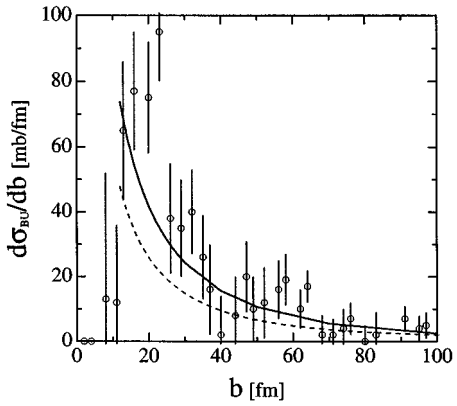

FIG. 5. The Coulomb breakup cross section as a function of the impact parameter b. The solid curve is the result of the present model, while the dashed curve is the result with the ls potential turned off [14]. Experimental data are from [8].

$V_p=-32.0$ MeV which locates the $0p$ excited state at $E=-0.183$ MeV. The latter case corresponds to the previous calculation in [14]. This was chosen because the $1/2^-$ excited state of ^{11}Be is known to have the strong $E1$ transition strength. The $B(E1)$ strength calculated with the l-independent potential is already presented in Fig. 2. When the resonance exists, the sharp peak appears at the resonance energy. Except for the energy region of the sharp peak, the $B(E1)$ strength is rather similar between the two cases of the resonance and the bound excited state. The $B(E1)$ strength function with the l-independent potential has also similar shape, although its magnitude is larger by a constant factor. This difference is understood by noting that, for the case of the l-independent potential, there is no resonant nor bound excited state in the p wave so that all the $E1$ strength appears in the continuum. The similarity in the shape of the $B(E1)$ strength for three cases indicates that the energy dependence of the nonresonant part of the $B(E1)$ strength is mainly determined by the wave function of the ground state, and is rather insensitive to the level structure of the excited states.

IV. ANALYSIS OF ^{11}BE COULOMB BREAKUP REACTION

In this section we analyze the Coulomb breakup reaction of $^{11}\mathrm{Be}+^{208}\mathrm{Pb}$ at the incident energy of 72 MeV/nucleon done at RIKEN [8]. To reproduce the known properties of the ^{11}Be structure, we choose the potential between the neutron and the ^{10}Be core nucleus in the following way: The depth V_0 is determined to reproduce the neutron separation energy of the ^{11}Be (0.503 MeV) by assuming the $1s$ orbit of the halo neutron. For $l\neq 0$ channels the central and ls potentials are included. The strength of the ls potential is set the standard value for the p-shell nucleus, $V_{ls}=32.8$ MeV fm^2. The strength of the central potential is then determined to reproduce the observed $1/2^-$ excited state located at -0.183 MeV from the neutron threshold. The state is assumed to be described simply with the $0p_{1/2}$ orbit. No deformation or clustering effect of the ^{10}Be core nucleus is taken into account. The values employed are $V_0=-58.3$ MeV and $V_p=-40.4$ MeV, respectively.

The time evolution of the wave function is calculated by using the same parameter sets as the previous section. The Coulomb breakup cross section is obtained by the integration over the impact parameter larger than $b_{\min}=12$ fm [see Eq. (10)]. The reaction of the impact parameters smaller than $b_{\min}$ proceeds by the nuclear force as well as the Coulomb force, and is assumed to lead to more violent nuclear reaction processes.

The Coulomb breakup process is dominated by the dipole component of the target Coulomb field, and proceeds through the excitation to two angular momentum channels, $j^\pi=1/2^-$ and $3/2^-$. The $B(E1)$ transition strength to the bound level of $1/2^-$ is calculated to be 0.251 e^2 fm^2 in the present model, which is considerably larger than the measured value, 0.115 ± 0.011 e^2 fm^2 [5]. The transitions to the other bound levels below the ground state, which should not occur in principle, are not excluded in the process of the time evolution of the wave function, but the mixing-in of those states is found to be negligible in the present calculation.

A recent experiment at GANIL [16] observed the Coulomb excitation to the $1/2^-$ state. The extracted $B(E1)$ transition strength is noticeably less than that determined from the lifetime measurement [5]. In order to see if higher order effects have some hint for this puzzling result, we compared the excitation probability to the state between the present model and the perturbation theory. The difference between the two calculations is not significant; about 20% larger at $b=12$ fm in the present model. This suggests that the higher order effect cannot explain the GANIL data. Another Coulomb excitation experiment has very recently been done at RIKEN to extract the $E1$ transition rate [17]. According to it the rate is consistent with that determined from the lifetime measurement.

We show in Fig. 5 the impact parameter dependence of the breakup cross section $d\sigma_{\mathrm{BU}}/db=2\pi bP_{\mathrm{BU}}(b)$. The calculated distribution is compared with the data [8] which are extracted from the measured breakup cross sections by using the classical argument for the trajectory. Figure 6 compares the energy spectrum of the breakup cross section, $d\sigma_{\mathrm{BU}}/dE$, with the measurement [8]. The calculation rea-

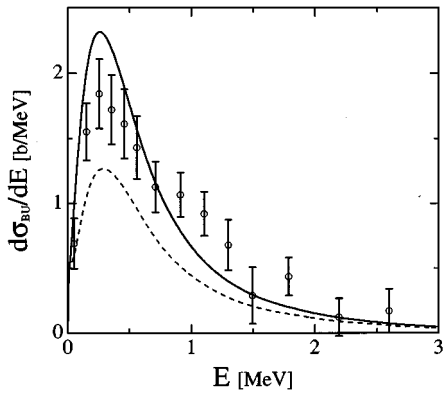

FIG. 6. The Coulomb breakup cross section as a function of the energy E of the relative motion between the neutron and the ^{10}Be nucleus. The solid curve is the result of the present model, while the dashed curve is the result with the ls potential turned off [14]. Experimental data are from [8].

sonably reproduces the measured distribution. Dashed curves in Figs. 5 and 6 show the previous results of [14] obtained without use of the ls potential, where the $0p$ orbit was fitted to the energy of the bound excited $1/2^-$ level. Since the $E1$ transition to this excited state, though fairly strong, does not lead to the breakup reaction, the breakup probability was underestimated in the previous calculation. By the introduction of the ls potential the $0p$ orbit now splits into two levels, $0p_{1/2}$ and $0p_{3/2}$, in the present calculation. Since the bound $0p_{3/2}$ orbit is located below the ground state and the transition to this state is small, most of the $E1$ strength in the $p_{3/2}$ channel is distributed in the continuum. This is the reason why the breakup cross section increased in the present model which includes the ls potential. The calculated $B(E1)$ strength function shown in Fig. 7 also confirms that the inclusion of the ls potential leads to the increase in the strength for the same reason mentioned above. The $B(E1)$ strength is compared to the experimental data which are extracted from the breakup cross sections by using the method of virtual photon spectra [18]. The agreement between theory and experiment is rather good, which is expected because the energy spectrum of the breakup cross section has already shown reasonable agreement as shown in Fig. 6. We note,

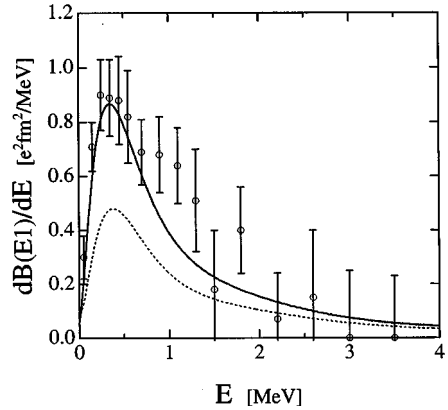

FIG. 7. The $B(E1)$ strength as a function of the energy E of the relative motion between the neutron and the core nucleus. Experimental data are from [8].

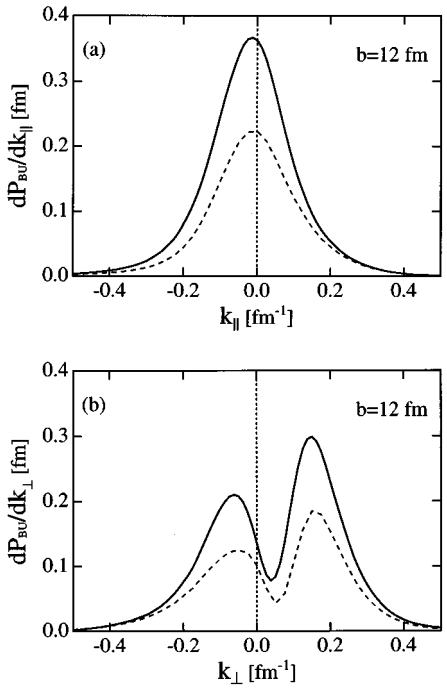

FIG. 8. The longitudinal (a) and transverse (b) momentum distributions of the relative motion between the neutron and the ^{10}Be nucleus. The impact parameter b is set 12 fm. The solid curve is the result of the present model, while the dashed curve is the result with the ls potential turned off [14].

however, that the present model overestimates the $B(E1)$ strength to the $1/2^-$ excited state, and do not know what effects the overestimation causes on the breakup mechanism.

We display in Fig. 8 the longitudinal and the transverse momentum distributions of the neutron-core relative motion. The impact parameter is set the smallest value, $b=12$ fm. The longitudinal momentum distribution is obtained by integrating the distribution of Eq. (9) with respect to k_x and k_y, while the transverse distribution is obtained by the integration over k_y and k_z. The longitudinal momentum distribution slightly shifts to the negative direction, whereas the transverse momentum distribution shifts to the positive direction. The average value of the momentum of the relative motion is $\langle k_\parallel \rangle = -0.019$ fm^{-1}, and $\langle k_\perp \rangle = 0.053$ fm^{-1}, respectively. The measured difference of the longitudinal momentum is about 0.04 fm^{-1}, which is close to the value of $k_c = 0.046$ fm^{-1} expected from the classical picture. Though the calculation reproduces a right order of magnitude, it explains only a half of the measured value.

Finally we consider the breakup mechanism referring to the result of the previous section. The mechanism is different in two channels, $j^\pi = 1/2^-$ and $3/2^-$, because they have different level structure of the excited states. In the $j^\pi = 1/2^-$ channel there is a bound excited state which is very close to the threshold. This situation is similar to the case of $V_p = -32.0$ MeV which we already investigated in Fig. 3 with the ls potential turned off. As expected, the momentum difference in this channel, especially in the longitudinal direction, is very small. On the other hand, there is no bound excited state in the $j^\pi = 3/2^-$ channel. The situation is thus similar to the case of $V_p = -45$ MeV in Fig. 3. The average longitudinal momentum difference increases and turns out to

be -0.022 fm^{-1}, about a half of the classical value of k_c. The breakup reaction of ^{11}Be is thus considered to occur in these two different mechanisms. Our previous treatment [14] which did not include the ls potential is equivalent physically to including only the former process. It is therefore understandable that we obtained the very small longitudinal momentum difference in that case. A realistic choice of the internal Hamiltonian, particularly the inclusion of the spin-orbit interaction, is very important for a quantitative analysis of the breakup reaction of the ^{11}Be nucleus.

V. SUMMARY

We investigated the Coulomb breakup mechanism of the nuclei with single neutron-halo structure, focusing on the mechanism which causes the momentum difference of the neutron-core relative motion after the breakup. The breakup process was described in the framework of the time-dependent Schrödinger equation by treating the target Coulomb field as a time-dependent external potential.

We first discussed the validity and the limitation of the classical arguments made for the postacceleration effect from the quantum-mechanical viewpoint by investigating the dependence of the reaction mechanism on the neutron binding energy and the level structure of the halo nucleus. We found that the classical arguments do not have quantitative accuracy though it is useful to understand the qualitative aspects of the quantum calculation. A behavior which cannot be understood in the classical picture occurred particularly when the bound excited state locates close to the neutron threshold. Small longitudinal and large transverse momentum differences were found in this case.

We analyzed the Coulomb breakup reaction of ^{11}Be+^{208}Pb by employing a realistic potential that describes the relative motion between the neutron and the ^{10}Be nucleus. A spin-orbit potential was included to describe the splitting of the structure of p states. The reaction proceeds through two channels, $j^\pi = 1/2^-$ and $3/2^-$. Since the $1/2^-$ channel has a bound excited state near the threshold but the $3/2^-$ channel does not have any bound excited states or low-lying resonances, the breakup mechanism is rather different in the two channels. By including the neutron-^{10}Be ls potential we took into account, in the present analysis, the difference in the breakup mechanism which is sensitive to the level structure of the nucleus. By this improvement the postacceleration effect was enhanced compared to the previous case which neglected the ls potential and moreover the magnitude of the energy spectrum of the fragments was in reasonable agreement with the measured values. The momentum difference in the longitudinal direction was, however, still underestimated by a factor of 2 compared with experiment.

ACKNOWLEDGMENTS

This work was supported in part by a Grant-in-Aid for Scientific Research (No. 0524102 and No. 06640381) of the Ministry of Education, Science and Culture, Japan.

[1] P.G. Hansen, Nucl. Phys. **A553**, 89c (1993).
[2] T. Kobayashi *et al.*, Phys. Lett. B **232**, 51 (1989).
[3] Y. Suzuki and Y. Tosaka, Nucl. Phys. **A517**, 599 (1990); G.F. Bertsch and J. Foxwell, Phys. Rev. C **41**, 1300 (1990).
[4] K. Ikeda, Nucl. Phys. **A538**, 355c (1992); P.G. Hansen and B. Jonson, Europhys. Lett. **4**, 409 (1987).
[5] D.J. Millener, J.W. Olness, E.K. Warburton, and S.S. Hanna, Phys. Rev. C **28**, 497 (1983).
[6] H. Kurasawa and T. Suzuki, Prog. Theor. Phys. **94**, 931 (1995).
[7] K. Ieki *et al.*, Phys. Rev. Lett. **70**, 730 (1993); D. Sackett *et al.*, Phys. Rev. C **48**, 118 (1993).
[8] T. Nakamura *et al.*, Phys. Lett. B **331**, 296 (1994).
[9] G. Baur, C.A. Bertulani, and D.M. Kalassa, Nucl. Phys. **A550**, 527 (1992).
[10] R. Shyam, P. Banerjee, and G. Baur, Nucl. Phys. **A540**, 341 (1992).
[11] S. Typel and G. Baur, Nucl. Phys. **A573**, 486 (1994); Phys. Rev. C **54**, 2104 (1994).
[12] L.F. Canto, R. Donangelo, A. Romanelli, and H. Schulz, Phys. Lett. B **318**, 415 (1993).
[13] (a) G.F. Bertsch and C.A. Bertulani, Nucl. Phys. **A556**, 136 (1993); Phys. Rev. C **49**, 2839 (1994); (b) H. Esbensen, G.F. Bertsch, and C.A. Bertulani, Nucl. Phys. **A581**, 107 (1995).
[14] T. Kido, K. Yabana, and Y. Suzuki, Phys. Rev. C **50**, R1276 (1994).
[15] S.E. Koonin, *Computational Physics* (Benjamin-Cummings, New York, 1986).
[16] R. Anne *et al.*, Z. Phys. A **352**, 397 (1995).
[17] T. Nakamura, private communication.
[18] J.D. Jackson, *Classical Electrodynamics*, 2nd ed. (Wiley, New York, 1975) p. 719.